THE MECHANISM OF HELA CELLS AS AN ANTICANCER DRUG BASED ON HAP NANOPARTICLES

Junsong Song, Borong Leng, Xuejun He*, Bingfeng Li, Rui Wang
College of Life and Health, Nanjing Polytechnic Institute, Nanjing, 210000, China

ABSTRACT

In order to investigate the mechanism of action of HAP nanoparticles on HeLa cells, the nano solution was prepared by HAP nanoparticles and mixed with the anticancer drug nicotine. The apoptosis degree of HeLa cells was detected using in situ terminal labeling method. The experimental data of each group in the experiment were analyzed by State7.0 software, and the mechanism of action of HAP nanoparticles on HeLa cells was investigated. The results showed that the nanoparticles with a diameter of 56.8nm could not only pass through the cytoplasm but also enter the nucleus. Therefore, HAP nanoparticles with a smaller diameter could enter the nucleus of HeLa cells by targeting and releasing the active anticancer drugs into the nucleus of HeLa cells to eliminate them. HeLa cells were induced by HAP nanoparticles. There was a strong dependence on the dose and time of HeLa cells and HAP nanoparticles. It could be concluded that reasonable selection of drug concentration and time could make HeLa cells exert a satisfactory apoptotic effect. SFSP significantly inhibited the proliferation of HeLa cells, and SFSP had a strong cytotoxic effect on HeLa cells.

Keywords: *TdT-mediated dUTP-biotin nick end labeling, apoptosis, HAP nanoparticles, HeLa cells, mechanism of action.*

DOI: 10.19193/0393-6384_2022_1_90

Received *March 15, 2021;* ***Accepted*** *December 20, 2021*

Introduction

Nanomaterials are ultrafine materials with nanometer grain size. The size of their particles is larger than that of atomic clusters and smaller than that of ordinary particles, generally 1-100nm[1]. Their surface effect, volume effect, and quantum size effect fundamentally change the structure of materials, making nanomaterials show many wonderful properties different from ordinary materials at the macro level. In 1984, Gleiter of Saarland University in Germany and Siegel of Argonne Laboratory in the United States successively succeeded in producing nanometer fine powder of pure matter. Gleiter prepared sintering nano-microcrystalline blocks through in situ pressure forming under high vacuum conditions, thus helping research on nanomaterials enter a more advanced stage. Therefore, nanomaterials science was officially declared as a new branch of materials science at the first International Nanoscience and Technology Conference held in the United States in July 1990[2]. The corresponding development of nanotechnology has been recognized as the most promising scientific research field in the 21st century. As an emerging science and technology with the most potential market application, its potential importance is beyond doubt. Some developed countries have invested

a lot of labor and funds in related research. For example, the United States was the first to establish a nano research center, and the Ministry of Culture, Education, Science and Technology of Japan listed nanotechnology as one of the four key research and development projects of materials science[3].

In Germany, where the University of Hamburg and the University of Mainz are nanotechnology research centers, the government spends $650 billion a year to support Microsystems research. In China, many scientific research institutes and universities have also organized scientific research forces to actively carry out research on nanotechnology and achieved certain research results, mainly as follows: the synthesis of directional carbon nanotubes array was completed by Researcher Xie Sishen et al., Institute of Physics, Chinese Academy of Sciences[4]. They efficiently produced carbon nanotubes with a diameter of about 20 nanometers and a length of about 100 microns using a chemical vapor process. The nanotube array was prepared with an area of 3 mm x3 mm and a space of 100 microns between carbon nanotubes.

At present, the research scope of nanobiology at home and abroad involves important fields such as nanobiology materials, drugs and nanobiology carriers, nanobiology sensors and imaging technology, and fine structure analysis of biomolecules using nanotechnology[5]. In nanobiological materials, nanoparticles can be widely used as a good contrast agent for medical imaging diagnosis. After shadow treatment, iron oxide particles are carried by the blood to various parts of the body and are absorbed by reticuloendothelial cells in the liver and spleen. The reticuloendothelial cells in the liver are composed of macrophages called Kupffer cells, which can engulf iron oxide particles; whereas malignant tumor tissue contains only a very small number of Kupffer cells and does not absorb iron oxide in large quantities[6]. Nanometer iron oxide contrast agent is used to spot the differences between the malignant tumor tissues and normal tissues to show the lesions. Diagnostic specificity of nanometer iron oxide, one by one in the number of normal and tumor tissues, can cause the difference in signal strength and the difference in magnetic resonance imaging, due to the normal tissue absorption of nanometer iron oxide characterized by dark low signal, it does not suck the collected nano ferric oxide and exhibits bright high signal. In this way, MRI images of lesions and normal tissues can have a large contrast[7]. Apoptosis is an urgent research hotspot in the field of life sciences. The study of apoptosis can deeply reveal many medical and biological mysteries such as immune response and embryo development, and clarify the mechanism of cell action and apoptosis of different diseases, which is helpful for the treatment of diseases[8]. To study the mechanism of action of HAP nanoparticles on HeLa cells, combine HAP nanoparticles with cancer drugs, and further study the mechanism of action of HAP nanoparticles on HeLa cells, in order to provide a theoretical basis for the treatment of cervical cancer.

Materials and methods

Materials and instruments

HeLa cells were provided by Tongpai (Shanghai) Biotechnology Co., Ltd; Hydroxyapatite (HAP) nanoparticles were provided by Wuhan Haineng Environmental Protection Technology Co., Ltd; Fluorouracil was provided by Shanghai Xudong Pharmaceutical Factory; 0.25% trypsin from Sigma company; Newborn calf serum from Hangzhou Sijiqing Institute of Bioengineering Materials; Rpmi-1640 culture medium of Wuhan Punosai Life Science And Technology Co., Ltd; Tunel kit from Beijing Baolaibo Technology Co., Ltd; Dimethyl sulfoxide (DMSO) from Shanghai Haoran Biological Co., Ltd; Phosphate buffer salt solution (PBS) of Shanghai Mingbo Biotechnology Co., Ltd; Epon812 kit of Haide Venture (Beijing) Biotechnology Co., Ltd; Fluorescein isothiocyanate (FITC) from Shanghai Yuanye Biological Co., Ltd.; Jem-arm300f GRAND ARM transmission electron microscope of Jieoulu (Beijing) Technology and Trade Co. Ltd; EVO MA 10/LS 10 Tungsten filament scanning electron microscope of Beijing Oubotong Optical Technology Co., Ltd; Electronic analytical balance of Shanghai Tianmei Balance Instrument Co., Ltd and Sodium hexametaphosphate from Shandong Zhenhua Industrial Co., Ltd.

Summary of preparation methods of HAP nanomaterials

The preparation methods of HAP nanomaterials can be divided into two categories: physical method and chemical method.

The physical method includes gas condensation method, sputtering method, etc., and the chemical method includes liquid method and gas-phase method. Nano inorganic materials are mainly prepared by the liquid phase method[9]. Here is a brief overview of these common methods.

Method of precipitation

A soluble salt solution including one or more ions, adding precipitant (such as OH-, $C_2O^{2-}_4$, CO^{2-}_3, etc.), or at a certain temperature to hydrolyze the solution, the formation of insoluble hydroxide or salt precipitation from the solution, and the original anions in the solution washed away, through thermal decomposition to obtain the desired nanoparticles. The precipitation method is divided into the coprecipitation method and the homogeneous phase precipitation method.

Coprecipitation method

The method of complete precipitation of all ions can be divided into single-phase co-precipitation and mixture co-precipitation after the addition of precipitant in a solution containing a variety of cations. The precipitation of single-phase co-precipitation consists of a single compound or single-phase solid solution. This method involves a narrow scope of application and strict control of conditions[10]. The precipitation products of the mixture co-precipitation are mixtures, and the process is very complicated. The precipitation of various ions is closely related to the pH value of the solution successively. In order to obtain the uniformity of precipitation, salt solutions containing a variety of cations are usually added slowly to the excessive precipitator and stirred to make the concentration of all precipitated ions exceed the equilibrium concentration of precipitation. Try to precipitate each component in proportion at the same time, so as to obtain a relatively uniform precipitate[11].

Homogeneous precipitation method

Like precipitation process, this method is also unbalanced, but if the concentration of precipitant in the solution is controlled to increase slowly, the precipitation in the solution is in equilibrium, and the precipitation can appear evenly in the whole solution. This method is called homogeneous precipitation. Generally, the precipitant is generated slowly by a chemical reaction in the solution, so as to overcome the local inhomogeneity of precipitant caused by adding precipitant to the solution from outside, resulting in the defect that precipitation cannot appear uniformly in the whole solution. In this way, monodisperse nanoparticles with small particle size can be prepared[12]. So far, HAP microcrystals have been obtained in CA-p salt solution using different systems. The method used is chemical precipitation method; the more commonly used systems are $Ca(OH)_2$-H_3PO_4-H_2O system, $Ca(NO_3)_2$-$(NH_4)HPO_4$-$NH_3{\cdot}H$-O system, $CaCl_2$-K_2HPO_4-KOH system, $CaHPO_4$-$Ca(PO_4)_2O$-H_2O system, etc. HAP microcrystals can be prepared by the above-mentioned systems, and the particle size can be smaller than 1 . The HAP microcrystals prepared by the neutralization reaction of the old $Ca(OH)_2$-H_4PO_4-H_2O system and the homogeneous precipitation reaction of $Ca(H_2PO_4)_2{\cdot}H_2O$-$Ca(OH)_2$ system do not carry impurity ions.

• The saturated $Ca(OH)_2$ solution was prepared by the neutralization reaction of $Ca(OH)_2$-H_3PO_4-H_2O system. The H_3PO_4 solution was slowly dropped into the solution and stirred continuously at the same time. The Ca/P molar ratio in the base apatite was controlled by the acidity meter. Apatite nanopowder prepared by this method is relatively pure, but it is difficult to make it stable[13].

• Uniform precipitation of $Ca(H_2PO_4)_2{\cdot}H_2O$-$Ca(OH)_2$ by adding $Ca(H_2PO_4)_2{\cdot}H_2O$ to saturated $HCA(OH)_2$ solution and stirring until the sol is stable, HAP particles with small size and monodisperse can be prepared by this method. The test results showed that HAP particles were needle-like crystals of 20nm×70nm and HAP particles were evenly distributed[14].

Alcohol brine solution

In this method, some metal-organic alcohol salts that can dissolve in organic solvents and may hydrolyze are used to form precipitation, a method to prepare nanopowder. This preparation method can obtain the same composition of particles[15]. For example, HAP nanoparticles can be prepared by this method. Using $Ca(EDTA)^{2-}$ hydrolysis reaction, the preparation process is as follows: Equimolar disodium ethylenediaminetetraacetic acid ($Na_2H_2{\cdot}EDTA$) and $CaCI_2$ were first dissolved in distilled water, then mixed with NaH_2PO_4 solution, and the pH value was adjusted to about 5 by NaOH. The mixture was sealed into a sodium borosilicate glass tube, immersed in silicone oil and kept at a constant temperature of 150°C, to obtain needle-like HAP nanoparticles[16]. The equation for the reaction process is as follows:

$$Ca(EDTA)^{2-} \rightarrow Ca^{2+} + EDTA^{4-} \quad (1)$$

$$10Ca^{2+} + 6PO_4^{3-} + 2OH^- \rightarrow Ca_{10}(PO_4)_6(OH)^-_2 \quad (2)$$

Spraying method

This method is a combination of chemistry and physics to obtain ultrafine particles by atomizing

the solution through various physical means. Its basic processes are preparation, spraying, drying, collection, and heat treatment of the solution. It is characterized by relatively uniform particle distribution, but the particle size is submicron to 10. The specific size range depends on the preparation process and spray method, for example, ultrafine particles of Al2O3 can be prepared by this method[17].

Hydrothermal method

The hydrothermal reaction is high-temperature and high-pressure water (aqueous solution) or steam and other fluids in the general term of the chemical reaction. Since 1982, the preparation of ultrafine powder by the hydrothermal reaction has attracted much attention at home and abroad. The ultrafine powder prepared by the hydrothermal method has a minimum particle size of several nanometers. At present, there are many examples of preparation of nanoparticles by the hydrothermal method[18].

Solvent volatile decomposition method

There are many preparation methods related to this aspect. The most widely used method for preparing highly active nanoparticles is freeze-drying, which atomizes the metal solution into small droplets and cools them into solid quickly.

Heat then sublimates and vaporizes the water in the frozen droplets, forming the inorganic salt of the solute. Ultrafine powder was synthesized by roasting. The freezing drying method is divided into three processes, i.e., freezing, drying, and roasting. The average particle size of HAP particles was prepared by this method in the Institute of Metal Research, Chinese Academy of Sciences is 40nm, which has the advantages of small particles, narrow particle size distribution and no agglomeration[19].

Sol-gel process

The Sol-gel method is a new process for preparing inorganic materials developed in the 1960s. Its basic principle is as follows: the metal alkyd or inorganic salt through hydrolysis, and then the solute polymerization gelatinization, and then the gel drying, roasting, finally get inorganic materials. The Sol-gel method is used not only to prepare nanoparticles but also to prepare nanoparticle films.

Its advantages and disadvantages are as follows:

• Good chemical uniformity because in the sol-gel process, sol is made from solution, so the chemical composition of colloidal particles and colloidal particles is completely consistent.

• High purity powder (especially multi - component powder) is prepared without mechanical mixing.

• Particle fine colloidal particle size is smaller than I00nm.

• The method can accommodate insoluble or non-precipitating components. Insoluble particles are uniformly dispersed in solutions containing components that do not precipitate, and the insoluble components are naturally fixed in the gel system by gelation. The finer the insoluble particles, the better the uniformity of the system.

• The sintering temperature of spherical gel particles after drying is low, but the sintering property between gel particles is poor, and the sintering property of bulk materials is not good.

• It shrinks greatly when dry.

Configuration methods and related performance tests

Culture and passage of HeLa cells

Rami-1640 medium containing 10% inactivated calf serum was prepared with 0.1% streptomycin and penicillin. HeLa cells were inoculated in different culture bottles at a concentration of 1×10^5, and cultured in an incubator with a CO_2 concentration of 5% and saturated humidity of 37°C. The experiment was conducted under the condition in which the passage time was set at 23 days and HeLa cells were in the logarithmic growth phase.

Preparation of HAP nanoparticles for anticancer drugs

Nimostine was selected as an anticancer drug and HAP nano sol was combined with the anticancer drug. The preparation process of HAP nanosol is as follows: 1.1L deionized water and 550mg HAP nanoparticles are weighed by an electronic analysis balance, and the two are fully fused. The fully fused solution is phacoemulsified for 15 minutes by adding 110mg sodium h6-metaphosphate stabilizer, and the concentration of HAP nanosol is 500m/L.

The obtained nanosol was sterilized at 120°C for 30 minutes by high-pressure steam, cooled after disinfection, and stored in 4°C environment for backup. During the experiment, the preparation of HAP nano sol was diluted with fresh culture medium to obtain 50mg/L, 100mg/L, 200mg/L, 300mg/L, 400mg/L, 500mg/L concentration of nano solution.

Transmission electron microscopy (TEM) was used to observe the dispersion characteristics, size and morphology of HAP nanoparticles.

HAP-properties of nanoparticles

According to Zetasizer 3000HS particle size analyzer, the particle size distribution of haP-nanoparticles mainly ranges from 40.1nm to 89.7nm, with an average particle size of 65.9nm, as shown in Figure 1.

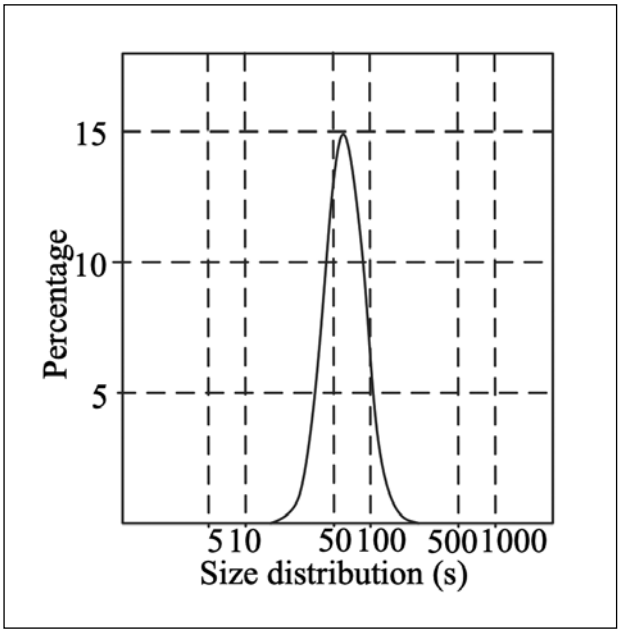

Figure 1: Particle size distribution and average particle size of HAP-nanoparticles sol.

The particle size distribution of HAP-nanoparticles mainly ranges from 40.1nm to 89.7nm, with an average particle size of 65.9nm.

As shown in Figure 2, TEM observation demonstrates that HAP nanoparticles are needle-like, evenly distributed, and well dispersed. TEM observation showed that no granular material was observed in the control sample (Figure 3A). In the experimental group, HAP nanoparticles between the two cells, which had not been phagocytosed into the cells, were found to be of needle-like structures and were mostly agglomerated together (Figure 3B).

This may be the result of the cancer cells condensing them together and allowing them to devour. Some cells extend their pseudopodia to separate HAP nanoparticles, surround them, and form end drinking bubbles for phagocytosis.

As can be seen in Figure 3C, HAP has entered the cancer cell and remained in the cytoplasm. No HAP nanoparticles were found in the nucleus. HAP nanoparticles agglomerate together, some of which are obviously agglomerated and the density is obviously increased, which is the concentration phenomenon after phagocytic foreign body.

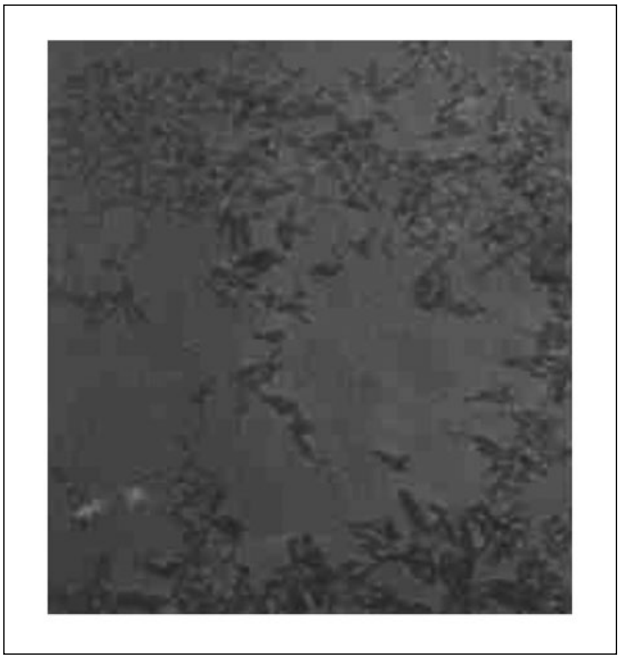

Figure 2: Transmission electron microscopy of HAP-nanoparticle sol.

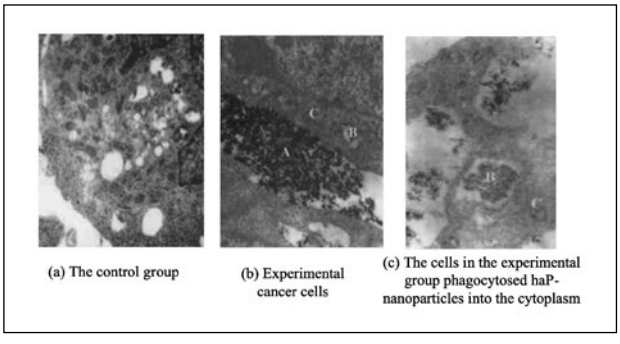

Figure 3: TEM observation of the control group and the experimental group.

Experimental study on

Data processing method

The experimental data were expressed in the form of, and the experimental data of each group in the experiment were analyzed statistically by State 7.0 software. The differences of the data were tested by T-test and ANOVA: when the experimental results were $P \geq 0.05$, there was no statistical significance of the experimental results, and there was no significant difference. When the experimental results were not $P<0.05$, there was a significant difference in the experimental results, which was statistically significant. When $P<0.01$, it indicated that there was a very significant difference in the experimental results, with statistical significance.

The effects of different particle sizes on endocytosis

FCM and GFAAS are important techniques to quantitatively evaluate the endocytosis efficiency of HAP nanoparticles. The specific surface area of HAP nanoparticles with different particle sizes is very different, so FCM cannot be used to evaluate the endocytosis performance of HAP nanoparticles.

The GFAAS method was used to measure the content of HAP nanoparticles in HeLa cells and evaluate the endocytosis rate of HAP nanoparticles. The number of HAP nanoparticles contained in HeLa cells under HAP particles with different particle sizes was counted, and the statistical results were shown in Figure 4.

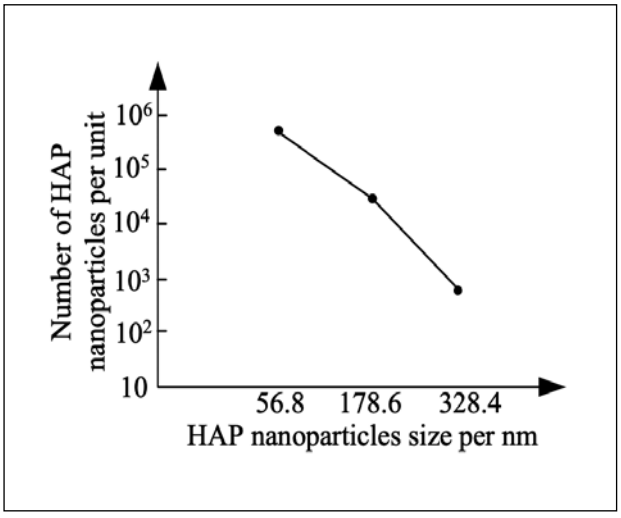

Figure 4: Number of HAP nanoparticles.

Experimental results show that the number of nanoparticles in HeLa cells acted by HAP nanoparticles with particle size of 56.8nm is significantly higher than that of HAP nanoparticles with particle size of 178.6nm and HAP nanoparticles with particle size of 328.4nm. The comparison results effectively verify that the endocytosis efficiency of HAP nanoparticles is significantly correlated with the particle size. The endocytic efficiency of HAP nanoparticles ranged from 56.8nm>178.6nm>328.4nm, respectively.

It was found that 56.8nm nanoparticles could penetrate the nuclear membrane of HeLa cells, which was consistent with previous reports. Nanoparticles with particle size of 56.8nm can not only pass through the cytoplasm but also enter the nucleus. Therefore, HAP nanoparticles with smaller particle sizes can enter the nucleus of HeLa cells by targeting action and releasing active anticancer drugs into the nucleus of HeLa cells to eliminate HeLa cells.

HeLa cells were inhibited by HAP nanosol at different concentrations

MTT assay was used to detect the proliferation inhibition rate of HeLa cells. The HeLa cells were cultured for 24h, 48h, and 72h by adding 5g/L phosphate buffer PBS at PH 7.5 each time. After adding phosphate buffer, culture was continued for 3.5h. After the culture, the culture medium was removed, and 140μL DMSO was added, and gently shaken for 10 minutes to dissolve blue-purple crystals. A value of the solution at 500nm was measured by a microplate reader.

The inhibition rate of cell proliferation was expressed as follows:

Cellular proliferation inhibition rate % = (A value of culture Medium-Experimental Group A value)/A value of culture medium×100%. The inhibition rates of DIFFERENT concentrations of HAP nanosol on HeLa cells were calculated, and the statistical results were shown in Table 1.

Concentration of HAP/(μg/ml)	24h	48h	72h
50	0.94±0.07	1.95±0.26	1.76±0.19
100	1.85±0.86	5.16±0.58	4.38±0.35
200	2.52±0.48	6.85±0.85	8.64±2.58
300	3.65±0.58	9.52±0.75	16.58±3.52
400	4.35±0.89	15.64±0.83	31.52±3.57
500	6.85±1.58	24.85±2.16	49.52±5.68

Table 1: Inhibition rates of DIFFERENT concentrations of HAP nanosol on HeLa cells.

The experimental results showed that the inhibition rate of HeLa cells increased with the increase in culture time, and the experimental results of each group were ALL $P<0.05$, showing statistically significant differences.

The inhibition rate of HeLa cells increased significantly, after 72h compared with 24h after HAP nano-sol mixed culture. The results showed that the inhibition effect of HAP nanoparticles at different concentrations on HeLa cells was obvious, and the inhibition rate increased with the increase in action time, indicating that the effect of HAP nanoparticles on HeLa cells was time-concentration dependent. The inhibition rate of HAP nanosol on HeLa cells increased with time.

HeLa cell results induced by HAP

The apoptosis degree of HeLa cells was detected by in situ terminal labeling method, and

the apoptosis detection process was performed according to the instructions of Tunel kit. The apoptotic HeLa cells that turned brown after the Tunel kit operation were identified as apoptotic HeLa cells. The low-power lens was set to contain 100 cells as the number of unit fields, 6 fields were selected, and the labeling index of apoptotic cells was the percentage of apoptotic cells. Six fields were selected under the low-power microscope, and 100 cells were selected in each field. Brown-yellow cells indicated that the cells had been apoptotic. The apoptosis rate of HeLa cells under different HAP concentrations was calculated, as shown in Table 2.

HAP/(μg/ml)	24h	48h	72h
Culture group	1.35±0.98	2.35±1.08	3.28±1.64
50	4.85±1.35	6.39±2.34	16.85±2.54
100	10.28±2.35	11.58±3.28	19.58±3.68
200	12.58±3.08	15.34±3.85	29.54±3.57
300	13.24±2.68	17.28±3.48	33.64±3.58
400	14.98±1.38	20.16±2.64	37.58±3.64
500	16.85±1.34	23.85±3.69	41.86±4.05

Table 2: Apoptosis rate of HeLa cells under HAP.

Table 2 Experimental results showed that HAP nanoparticles significantly induced HeLa cell apoptosis, and HeLa cell apoptosis was normally distributed with changing HAP nanoparticles concentration and time. The principle of cell apoptosis detection by the Tunel method is to mark the broken double-stranded DNA formed in the process and function of cell apoptosis by the end, which has a high level of differentiation between necrotic cells and apoptotic cells. Tunel positive cells and their nuclei showed morphological characteristics of apoptotic cells in crescent shape, granular shape, and ring shape. It was verified that morphological characteristics and positive distribution characteristics of apoptotic cells could be displayed simultaneously by Tunel staining. Because some cells belong to the early stage of apoptosis, some Tunel positive cells did not have significant morphological characteristics of apoptosis.

HAP nanoparticles can induce HeLa cell apoptosis, and the degree of HeLa cell apoptosis is significantly affected by the concentration of HAP nanoparticles and the time of action. When the concentration of HAP nanoparticles was low, HeLa cells were less affected by HAP nanoparticles, and the apoptosis rate of HeLa cells was higher than that of the culture medium group, with a statistically significant difference ($P<0.05$). The apoptosis rate of HeLa cells increased with increasing the concentration of HAP nano-sol, which was significantly different from that of 50μg/ mL HAP nano-sol. When the concentration of HAP nanosol was 400μg/ mL and 500μg/ mL, the apoptosis of HeLa cells was significantly different from that of other groups, and the statistical results were $P<0.01$. The experimental results effectively verified that HeLa cells were significantly induced by HAP nanoparticles, and there was a strong dependence on the dose and time of HeLa cells and HAP nanoparticles.

It was concluded that reasonable selection of drug concentration and time could achieve the satisfactory apoptotic effect of HeLa cells.

The inhibitory effect of SFSP on HeLa cells

HeLa cancer cell lines W in logarithmic growth phase were inoculated into 6-well plates with a concentration of 1.5 mL per chemical at 2×10^5 cells per well. After incubation overnight in an incubator containing 5% CO_2 at 37°C, SFSP dissolved in DMSO was added to the drug administration group to make the final concentration of 2, 5 and 10ng/ml, respectively, and only a blank control group called DMSO was added, with 3 multiple Wells in each group. Caspase-3, -8 and -9 activation ELISA kits were used to determine the activation of Caspase, and the 0D value at 405nm was measured with a microplate reader.

SFSP dose (*μg/ml*)	SMMC-7721 survival rate(%)			Bel-7404 survival rate(%)		
	24h	48h	72h	24h	48h	72h
0	100±0.00%					
0.625	92.65± 1.21%	81.46± 1.31%	68.01± 0.70%	98.65± 1.86%	93.35± 0.42%	83.47± 2.42%
1.25	85.60± 2.14%	63.10± 1.47%	40.23± 0.38%	92.31± 1.11%	73.80± 1.34%	35.67± 1.27%
2.5	68.13± 1.08%	18.92± 1.83%	9.52± 0.38%	78.46± 2.47%	23.47± 0.67%	8.68± 1.04%
5	30.96± 2.79%	9.56± 1.02%	6.04± 0.61%	33.51± 1.31%	8.87± 1.87%	7.43± 1.59%
IC50 (*μg/ml*)	3.75	1.56	0.95	3.93	1.77	1.10

Table 3: Inhibition of SFSP on HeLa cell proliferation ($\bar{x}\pm s$, n=4).

As can be seen from Table 3, SFSP had a significant inhibitory effect on HeLa cells, SMMC-7721 and BEL-7404, with a time-dependent and dose-dependent effect (P). SFSP significantly inhibited the proliferation of SMMC-7721 cells, with IC50 values of 3.75, 1.56 and 0.95 at 24h,48h, and 72h, respectively. The inhibition rates of SFSP5 dose group at 24h,48h, and 72h were 69.04%, 90.44%,

and 93.96%. SFSP also showed similar proliferation inhibition in another strain of HeLa cells. Its IC50 values at 24h, 48h and, 72h were 3.93, 1.77 and 1.10 , 5 , respectively. SFSP inhibition axis of BEL-7404 at 24h, 48h, and 72h reached 66.49%, 91.13%, and 92.57%. These results indicated that SFSP had a strong cytotoxic effect on HeLa cells.

Conclusion

In this paper, we proposed a method of HeLa cell action mechanism based on HAP nanoparticles. The nanoparticles were prepared by HAP nanoparticles and mixed with nicotine, and the apoptosis degree of HeLa cells was detected by in situ terminal labeling method. State7.0 software was used to analyze the experimental data of each group and analyze the mechanism of action of HAP nanoparticles anticancer drug on HeLa cells.

The following conclusions are drawn from the experiment

Nanoparticles with a particle size of 56.8nm can not only pass through the cytoplasm but also enter the nucleus. Therefore, HAP nanoparticles with a smaller particle size can enter the nucleus of HeLa cells by targeting action and releasing active anticancer drugs into the nucleus of HeLa cells to eliminate HeLa cells. The effect of HAP nanoparticles at different concentrations on HeLa cells was obvious, and the inhibition rate increased with the increase in action time, indicating that the effect of HAP nanoparticles on HeLa cells was time-concentration dependent.

HeLa cells were significantly induced by HAP nanoparticles, and there was a strong dependence on the dose and time of HeLa cells and HAP nanoparticles. It could be concluded that reasonable selection of drug concentration and time could achieve the satisfactory apoptotic effect of HeLa cells. SFSP significantly inhibited the proliferation of HeLa cell SMMC-7721, with IC50 values of 3.75, 1.56, and 0.95 at 24h, 48h, and 72h, respectively. The inhibition rates of SFSP5 dose group at 24h, 48h, and 72h were 69.04%, 90.44%, and 93.96%. SFSP also showed similar proliferation inhibition in another strain of HeLa cells. The results showed that SFSP had a strong cytotoxic effect on HeLa cells.

References

1) Li F., Chen X.D., Wang G.W., Li M., Wang J.L., Analysis on the studies of trend and hot spots of radiosensitivity for cervical cancer, Journal of Preventive Medicine Information, 2019, 35(10), 1178-1184.
2) Tian J., Lou X.L., Yao L., Zhang X.H., Effects of hyperbaric oxygen combined with vinblastine on the anti-cancer activity against human cervical cancer HeLa cells, Chinese Journal of Nautical Medicine and Hyperbaric Medicine, 2019, 026(006), 525-528.
3) Xiao M.F., Lu Z., Chen L.Y., Chen F., Effects of luteolin on proliferation and apoptosis of HeLa cells by regulating JAK2 / STAT3 signaling pathway, Chinese Traditional Patent Medicine, 2020, 42(6), 1620-1623.
4) Yang W.S., Chen S.H., Sun S., Liu C.J., Sheng Q.Y., Pan Y., Xuan Y.H., Molecular mechanisms of parthenolide on the Human Cervical Cancer Gela Cell Line Growth and Migration, International Journal of Geriatrics, 2017, 038(006), 241-245.
5) Bi J.Y., Li H., Wang H., Mechanism of bitter substances in citrus on proliferation and apoptosis of HeLa cells, Food Science, 2019, 40(19), 33-59.
6) Zhang L.L., Effects of serum on the endocytosis of integrin αvβ3 receptors in HeLa cells, Journal of Jining Medical College, 2017, 16(3), 66-79.
7) Zhao S.C., Zheng G.C., Huang L.Z., Zhong J., Wang B.Y., Chen S.F., Chen Z.S., Comparison of anti-cancer capacity of perinatal mesenchymal stem cells conditioned medium from three different sources, Journal of Modern Oncology, 2019, 27(11), 30-35.
8) Li J.F., Zhang Q.R., Fu Y.F., Li S.Y., Liu Y.L., Zhou J., Cai M.J., Yang G.C., Shan Y.P., Study on cytotoxicity of nano-drug carrier-polyamidoamine dendrimers, Chinese Journal of Analytical Chemistry, 2021, 49(6), 999-1007.
9) Zhang M.F., Shen Y.Q., Research progress of pharmacological effects of Matrine on cervical and endometrial cancer, Anti-Infection Pharmacy, 2019, 14(6), 78-89.
10) Tang Z.Y., He D.Y., Sheng M.J., et al. Antitumor effect of metformin on cervical cancer HeLa cells in vitro, Chinese Journal of Laboratory Diagnosis, 2018, 022(006), 1054-1058.
11) Zhong R., Wu S.W., He X.M., Long H., Xuan J.C., Liu H.Q., Antitumor Activity and Mechanism of Exopolysaccharide from Dunaliella salina, Science and Technology of Food Industry, 2020, 41(22), 126-133.
12) Li S.L., Wang C., An Y.N., Li Y., Wang X.Y., Tang X.D., Yu L., Mechanism of ROS increasing induced by PMA in HeLa cells, Chinese Journal of Cancer Prevention and Treatment, 2018, 25(09), 622-627.
13) Tang M.R., Wang J., Zhuo J.Z., et al., Morphological study on inhibition of HeLa cell proliferation by heteroscorpion toxin, Chinese Journal of Economic Zoology, 2018, 22(001), 1-5.
14) Wei Z.B., Ma L., Liu S., Liu Z.Q., Shi Y., Qu X.B., In vitro screening of anti-cancer agents from traditional Chinese medicine using the HeLa cell proliferation inhibition model coupled with Centrifugal Ultrafiltration Mass Spectrometry, Journal of Chinese Mass Spectrometry Society, 2017, 38(4), 494-502.
15) He Y.C., Xue H., Effects of 4 flavonoids from Scutellaria baicalensis on different cancer Cell lines, World Science

and Technology-Modernization of Traditional Chinese Medicine, 2017, 18(11), 1845-1854.
16) Du C.S., Ma Y.N., Wang S., et al., Study on reversal effects of levoshikonin on cisplatin resistance of Human Cervical Carcinoma HeLa Cells, China Pharmacy, 2020, 31(15), 1867-1873.
17) Cai F., Xue F., Zhu Y.H., et al., The role of multi-functional delivery system based on gold nanomaterials in the treatment of liver cancer, Chinese Journal of Experimental Surgery, 2019, 36(5), 844-848.
18) Jian M.C., Zhou X., Li H., Microrna-145 inhibits the occurrence and invasion of cervical cancer stem cell tumors, Journal of Hubei University of Medicine, 2018, 37(01), 14-23, 2.
19) Zhang B.Y., Yin X.C., Lin Y.H., et al., Research progress on the toxicity mechanism of zinc oxide nanoparticles and anti-cancer, Journal of Toxicology, 2019, 33(02), 157-161.

Corresponding Author:
Xuejun He
Email: HXJ1969njpi@126.com
(China)